ORIGINAL ARTICLE

Outbreak of a Tornado with Tropical Cyclone Yaas (2021) Formed over the Bay of Bengal

Nasreen Akter[1] (ORCID) · M. Rafiuddin[1]

Abstract

A tornado outbreak occurred in West Bengal (WB), India, about 15–16 h before the landfall of Cyclone Yaas formed in May 2021 over the Bay of Bengal. High-resolution analysis data have been used to investigate the possible tornadoes in terms of environmental conditions connecting to the cyclone. The WB tornado is found as intense as EF2–3 on the tornado scale and is likely associated with a mini-supercell. The total shear of 37 m s^{-1} from 0–6 km above ground level (AGL) with strong clockwise rotation, the moderate instability (1504 J kg^{-1}) and the energy helicity index of 2.2 are the substantial convective parameters related to the WB tornado. Moreover, the favorable environment owning intense bulk shear, a larger value of storm-relative environmental helicity in the lowest 1 km AGL and high values of significant tornado parameter (STP) urge the potentiality of multiple tornadoes spawning in multi-days accompanying the landfalling Cyclone Yaas. The right-front quadrant of the cyclone is found to be more vulnerable for developing moderate to severe tornadoes within its rainbands. The positive potential vorticity anomalies evidence the cloud-scale cyclonic circulation from surface to 400 hPa with the maximum in the mid-level.

Keywords Tornado · Supercell · Tropical cyclone · Bay of Bengal

1 Introduction

A tropical cyclone (TC) 'Yaas' formed on 23 May 2021 over the Bay of Bengal (BoB) and made landfall on the Odisha and West Bengal coasts of India on 26 May 2021 as a very severe cyclonic storm. During landfall, the TC attained its maximum intensity with a wind speed of 75 kt recorded by the India meteorological department (IMD). The estimated death toll of at least ten people in the low-lying coastal areas, but the damage scenario was catastrophic with destroying more than 46,900 houses, 2333.17 sq km of crop fields, 55.99 sq km of shrimp farms and fish cultivation area. (ACAPS 2021; IFRC 2021). Around 13 million people were affected in India and Bangladesh due to the slamming of Cyclone Yaas (2021) as well as 1–2 m higher tidal surfs

than the usual one. Moreover, at approximately 15–16 h before the center of the TC hit the land, a sudden tornado was reported swirling over villages of West Bengal (WB), India (Fig. 1a), and killed two people and damaging around 40 houses (Hindustan Times 2021; India Blooms 2021).

Most of the TCs making landfall in the United States and Japan have spawned tornadoes due to the development of extensive vertical wind shear and instability over the land (Fujita et al. 1972; Novlan and Gray 1974; McCaul 1991). In the duration from 1950 to 2007, the 1800 TC-tornadoes were enumerated in the continent of the United States (Moore and Dixon 2015). Among them, Hurricane Ivan (2004) causes a multi-day outbreak of 118 tornadoes (Moore et al. 2017). Many TC-tornadoes occur within 100 km on the coast during 12 h of landfall, but some are produced even further inland and days after landfall enduring more extensive paths with more vigorous intensity (Fujita et al. 1972; Weiss 1985; Moore et al. 2017).

The TCs coupled with tornadoes can have more devastation than a regular TC, especially for densely populated countries like Bangladesh and India, because strong downburst winds, hail, lightning, etc. are the additional dangerous aspects of tornadoes. According to the National Weather Service of the United States, the winds of a tornado can

---

Responsible Editor: Christian Franzke

✉ Nasreen Akter
  nasreenakter@phy.buet.ac.bd

1   Department of Physics, Bangladesh University
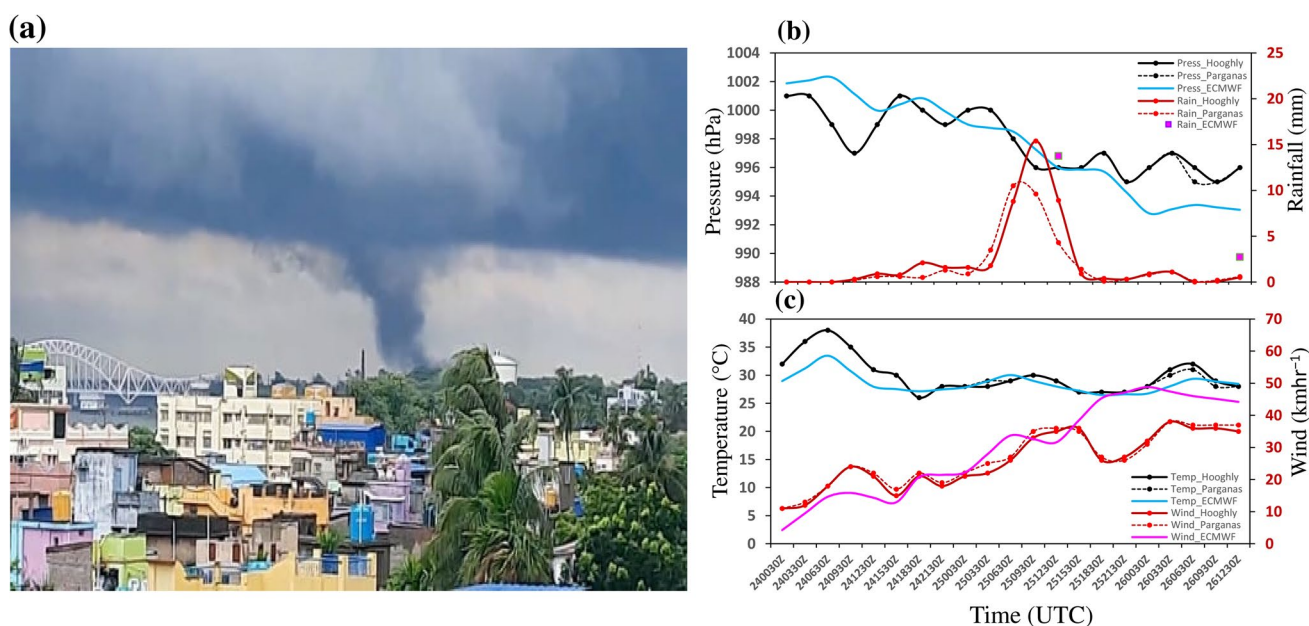   of Engineering and Technology (BUET), Dhaka, Bangladesh

Fig. 1 **a** Tornado outbreak in West Bengal, India on 25 May 2021 (Source: The Hindustan Times, 26 May 2021). **b** Time-pressure (primary axis) and time-rainfall (secondary axis) graphs **c** Time–temperature (primary axis) and time-wind (secondary axis) graphs for Chinsurah, Hooghly district (88.39°E, 22.90°N), Halisahar, the North 24 Parganas district (88.42°E, 22.93°N), West Bengal, India and ECMWF extracted values at 88.4°E, 23°N from 0030 UTC on 24 May 2021 to 1230 UTC on 26 May 2021

reach 483 km hr^{-1} with a damage path of more than 1.6 km wide and 80.5 km long (https://www.weather.gov/phi/TornadoDefinition). The earlier studies have shown that regular tornadoes (i.e., tornadoes formed in the absence of TCs) in Bangladesh during the premonsoon season (March–May) are responsible for more than 3500 deaths within 25 years from 1981 to 2005 (Bikos et al. 2016) and massive damage of properties (Ono 1997; Yamane et al. 2009). However, no study has been conducted so far regarding TC-tornadoes in the coastal countries of the BoB. As a result, associated awareness of tornadoes adjacent to TC is completely missing from the decision-making mechanism of the policymakers. General people do not even identify or classify the tornadoes that spawn during the landfall of TCs. Therefore, it is an utmost imperative task to comprehend and analyze the tornadoes associated with landfalling TCs that formed over the BoB. Due to the scarcity of radar data or high-resolution spatial and temporal data, the detailed cloud-scale structure of the tornado developed in WB, India before Cyclone Yaas (2021) hit the land is not practicable. Hence, the objective of the study is to investigate the atmospheric conditions for the WB tornado and the tornadoes that are anticipated to form after landfall. At this juncture, the overall severity and consequences of TC coupled tornado necessitate at least to be an eye-opener for the concerned authorities to make contingent steps to save lives and properties. In addition, this study will provide an assessment of the synoptic-scale atmospheric condition of shear, helicity and instability related to

the TC-tornadoes formed over the moist environment of the BoB and a comparison can be made with the environment of TC-tornadoes in other ocean basins (McCaul 1991).

To fulfill the objective, the horizontal data of 9 km resolution is used in this study because both the environment of tornadoes and the synoptic-scale environment of TC are essential and need to be incorporated. Mentionable that Mills and Colquhoun (1998) showed that the regional model of 80 km resolution could resolve sufficient detail of the kinematic and thermodynamic structure of the atmosphere to identify atmospheric environments for developing severe storms; even a tornadic thunderstorm environment can be accurately predicted. In a recent study, Koch et al. (2021) calculated the atmospheric instability and helicity conducive to severe thunderstorms using North American regional reanalysis data of 32 km resolution. Therefore, the data resolution used in this study is sufficient to explain together with the synoptic environment of a TC and the tornadoes embedded in it. The detailed structures of tornadic thunderstorms are beyond the scope of the paper.

2 Data Used and Validation

Due to the lack of observation data, the high-resolution global analysis data were considered for investigating the potential environment to develop tornadoes into Cyclone Yaas (2021). The European Centre for Medium-Range Weather Forecasts (ECMWF) with the Integrated Forecast System (IFS) CY41r2 6-hourly surface and isobaric atmospheric analysis data with a

horizontal resolution of 9 km (Malardel et al. 2015) were used in the present study. In the IFS, many meteorological fields, i.e., the horizontal wind, the virtual temperature and the surface pressure, were transformed to spectral space and back to grid-point space at every time step. A cubic grid was used instead of a linear arrangement for increasing the number of grid points. The isobaric data had 25 vertical layers with a top level of 1 hPa.

The 3-hourly surface data of temperature, wind, rainfall and pressure were collected for two stations, i.e., Chinsurah, Hooghly district (88.39°E, 22.90°N) and Halisahar, the North 24 Parganas district (88.42°E, 22.93°N), WB, India where the WB tornado was reported. The 6-hourly ECMWF data were extracted for the station point of 88.4°E & 23°N and compared with the observed trend lines of surface parameters in Fig. 1b and c for the period of 0030 UTC on 24 May 2021 to 1230 UTC on 26 May 2021. The mean differences in pressure, temperature and wind are around 0.36 hPa, 1.2 °C and 4.6 km hr^{-1}, respectively. The rainfall data of ECMWF are the 12-h forecast data plotted at 1200 UTC on 25 May 2021 and 1200 UTC on 26 May 2021 in Fig. 1b. The rainfall values are found to be almost similar to the observed data.

In addition, HIMAWARI-8 satellite images with surface precipitation data from the Integrated Multi-Satellite Retrievals for GPM (GPM IMERG) were used in this study (Fig. 2a) collected from https://www.nrlmry.navy.mil/TC.html. The GPM IMERG data has a spatial and temporal resolution of 10 km and 30 min, respectively.

For the validation of the TC track, the locations of Cyclone Yaas (2021) were extracted 6-hourly with respect to the minimum pressure from ECMWF analysis data and compared with the IMD best track data commencing from 0600 UTC on 23 May 2021 as shown in Fig. 2b. Both the tracks are tracing similar routes with a mean error of ~5 km. At the time of landfall (0000 UTC on 26 May 2021), the mean sea level pressure was 970 hPa for both cases.

Due to a lack of in-situ sounding data, the environments supporting the WB tornado were challenging to verify. However, the available sounding data of Calcutta (88.45°E, 22.65°N), WB, India collected from the University of Wyoming (https://weather.uwyo.edu/upperair/sounding.html) are shown here for 0000 UTC and 1200 UTC on 25 May 2021 and made a comparison in Fig. 3 with the Skew-T log-P diagrams obtained from ECMWF analysis data. All convective parameters are nearly the same in values except convective available potential energy (CAPE) at 1200 UTC on 25 May 2021. The observed CAPE of 2492 J kg^{-1} was larger than the analysis data attaining 905 J kg^{-1}. In both cases, the hodographs with unidirectional shears, the strong values of helicity, storm speeds and storm directions are similar suggesting the existence of a supercell thunderstorm.

3 Environment Associated with TC-Tornadoes

Tornado usually has a diameter on the scale of 100 s meters and is developed from a well-organized thunderstorm called a supercell (Moller et al. 1994). A supercell thunderstorm characterized by a deep rotating updraft
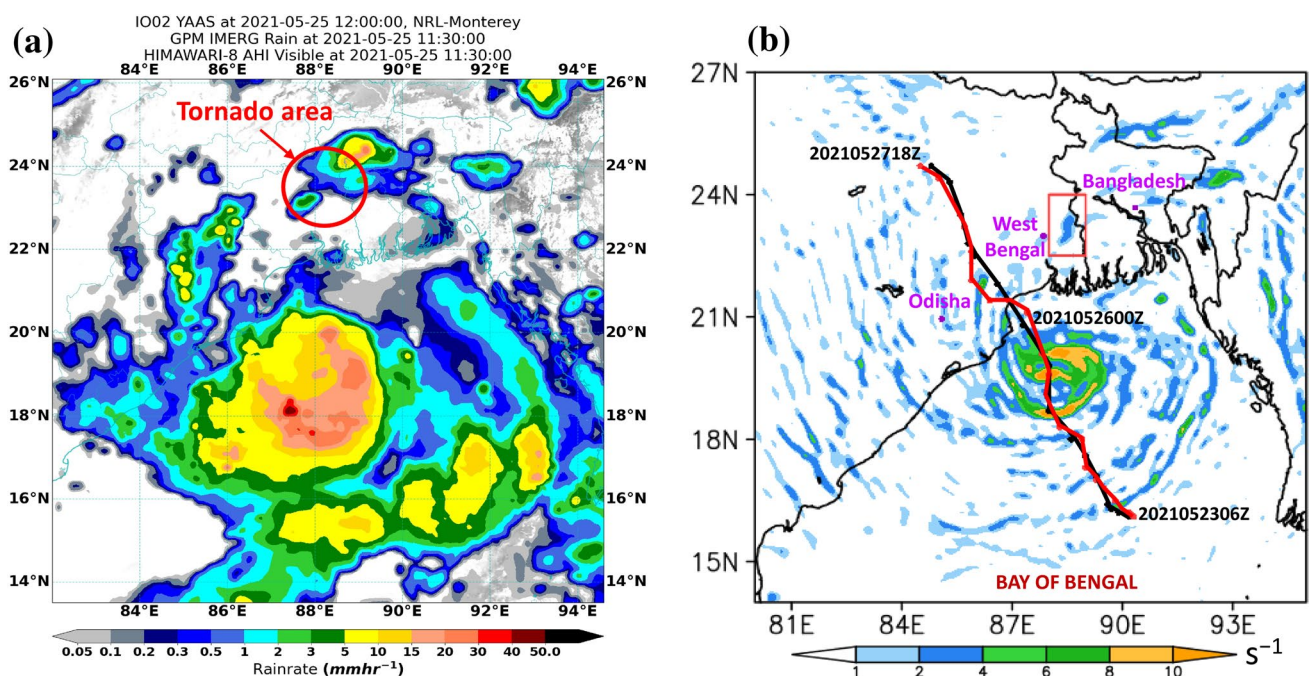

Fig. 2 **a** Satellite image of rainfall rate (mm hr^{-1}) for Cyclone Yaas at 1130 UTC on 25 May 2021. Circle indicates the tornado spawn area. **b** Relative vorticity (shaded; ×10^{-4} s^{-1}) at 900 hPa for 1200 UTC on 25 May 2021. Tracks of Cyclone Yaas are presented from 0600 UTC on 23 May 2021 to 1800 UTC on 27 May 2021 using IMD (black line) and ECMWF (red line) data
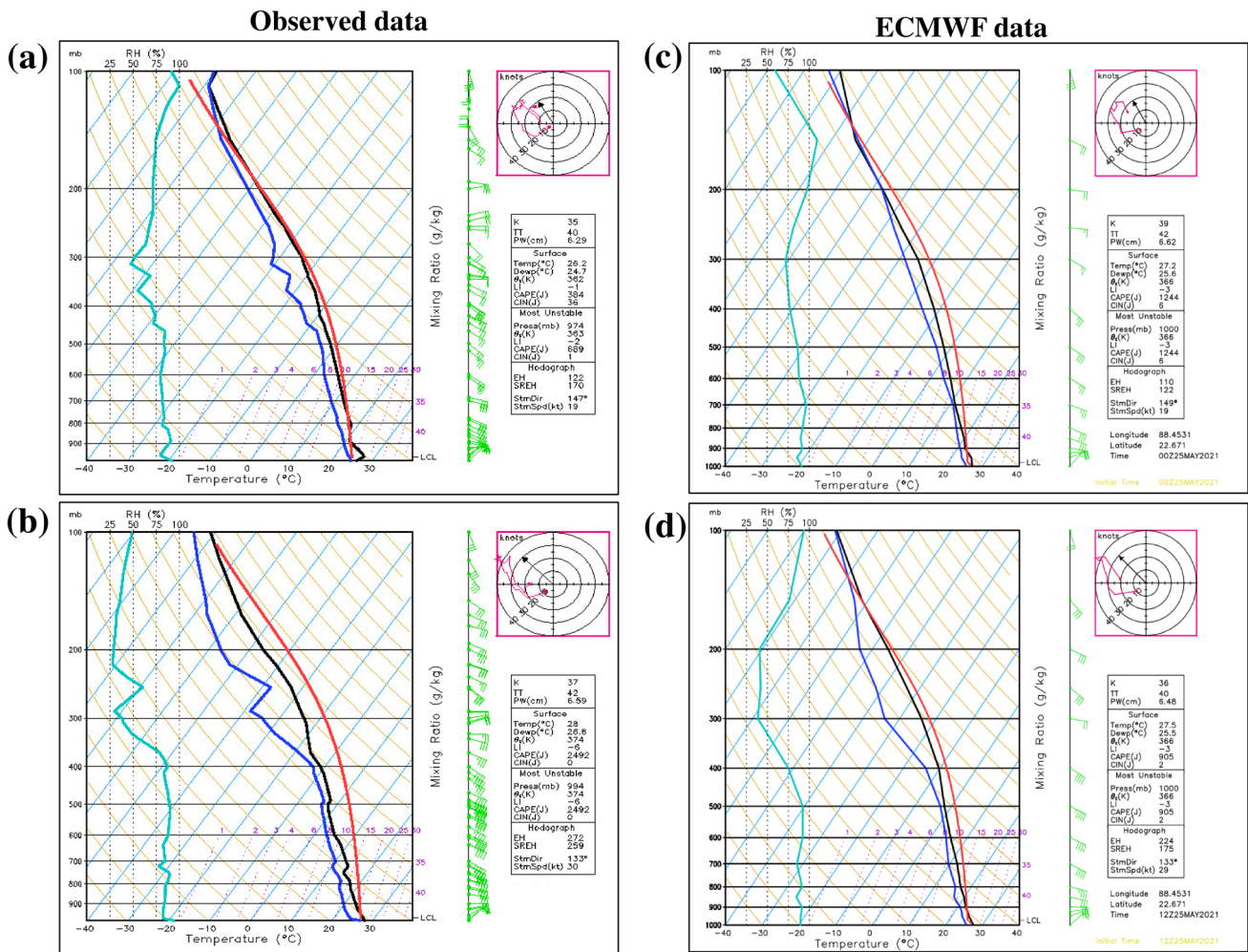
Observed data

ECMWF data

Fig. 3 Comparison of Skew-T log-P diagrams, wind barbs (in kt) and hodograph at Calcutta, West Bengal, India (88.45°E, 22.65°N) between the observation and ECMWF extracted data. **a** and **c** for 0000 UTC on 25 May 2021 **b** and **d** for 1200 UTC on 25 May 2021

(mesocyclone) evolves in a vertically sheared ambient environment. Low-level moderate-to-strong vertical wind shear, helicity and moderate-to-high instability are conducive to tornado development in a supercell. The environmental conditions related to the WB tornado are examined and additionally, monitoring the environment for the possibility of more tornadoes while TC is passing through the land.

3.1 The WB Tornado Outbreak

The WB tornado was observed at about 1130 UTC on 25 May 2021 at Chinsurah, Hooghly district and Halisahar, the North 24 Parganas district, WB, India around the position of 88.4°E, 23°N (India Blooms 2021). The abrupt increase of wind by 7–9 km hr^{-1}, rainfall by 7 mm and surface temperature by 1 °C, and decrease of pressure by 2 hPa are

noticed in Fig. 1b and c, which indicate the occurrence of severe weather between the time of 0930 UTC to 1230 UTC on 25 May 2021. The WB tornado was developed almost 380 km far away from the TC center. The location of the tornado is roughly marked in Fig. 2a, which relates to isolated convection in the rainband of Cyclone Yaas (2021) reaching the land before the eye of the TC. The rainbands of the TC mostly contain cloud clusters with isolated deep precipitating convective cells (rainfall rate of ~40 mm hr^{-1} in Fig. 2a) and associated storm-scale mesovortices. The mesovortices are the vortices at the meso-γ-scale which have the range of 2–20 km in diameter (Orlanski 1975) and are usually found in convective storms like squall line, bow echo and supercell thunderstorms (Weisman and Trapp 2003). The relative vorticity at 900 hPa for 1200 UTC on 25 May 2021 is depicted in Fig. 2b, which confirms several mesovortices in the rainbands spinning with an intensity of ~10^{-3} s^{-1}.

Previous studies have also noticed the development of meso-vortices within the convection in the rainbands of TCs due to vertical shear ensuing from the non-uniform wind flows over the BoB. Some mesovortices have the characteristics of mesocyclones with stronger updrafts evolving in the super-cell embedded in the rainbands of TCs in the BoB (Akter 2015; Akter and Tsuboki 2010).

Considering the occurrence time and location, the meso-vortex connected with the WB tornado is indicated in Fig. 2b and its vertical cross-section at 23.4°N is displayed in Fig. 4. The intense rotation (0.3×10^{-3} s^{-1}) in the lower level and

strong updraft (maximum of -4 Pa s^{-1}) up to 200 hPa are evident in Fig. 4a. The low-level convergence of horizon-tal winds having intense values of -4×10^{-5} s^{-1} (Fig. 4b) causes air to rise and induce deep vertical motion. The zonal component of wind along with vertical velocity shows the rising and rotating wind from the surface to the 400-hPa pressure level. In addition, the vertical distribution of equivalent potential temperature (θe) in Fig. 4b decreasing with increasing height represents convective instability up to 500 hPa. The atmospheric condition linked to the tor-nado is evaluated with Skew-T log-P diagram and hodograph
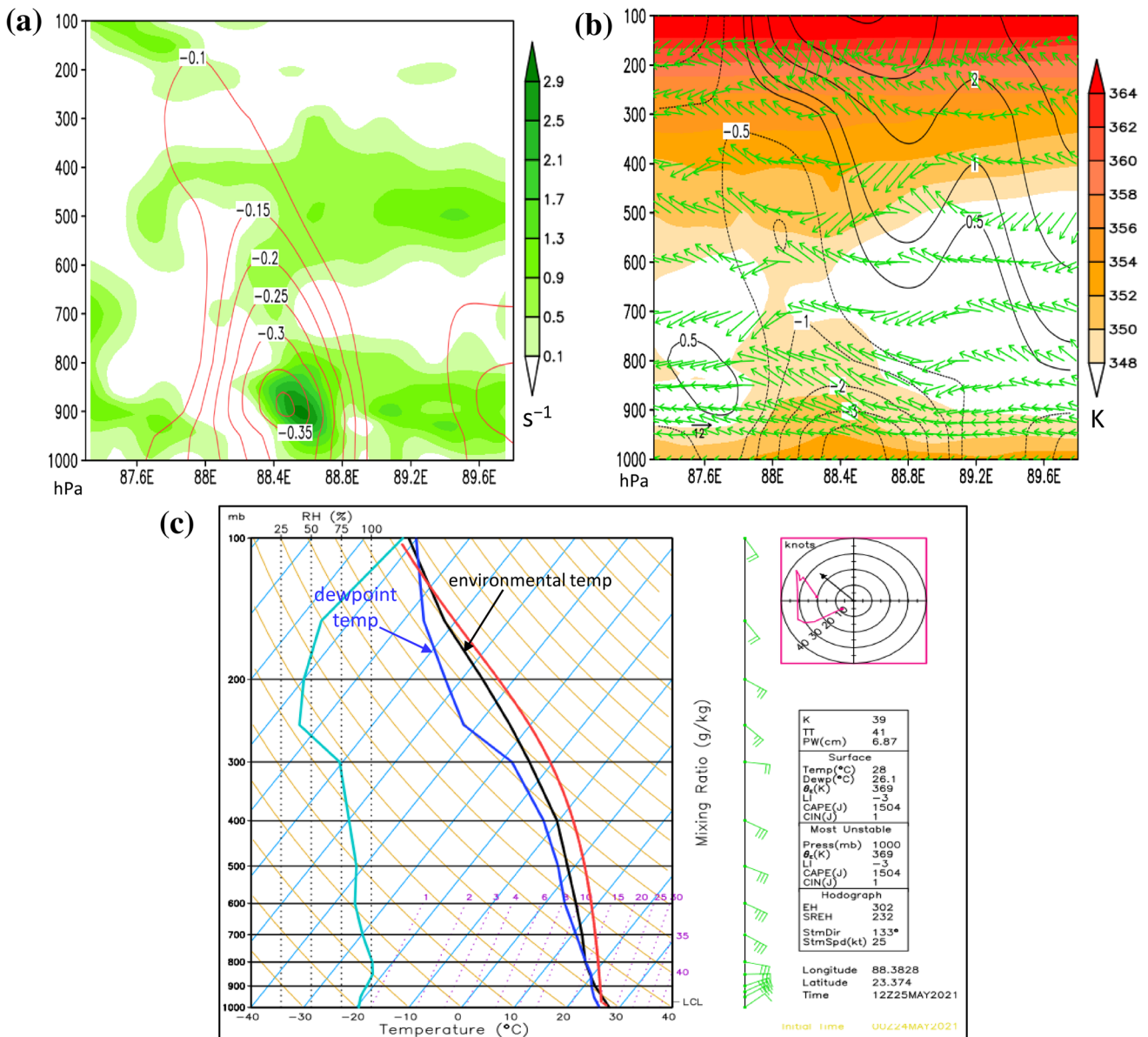

Fig. 4 Vertical cross-section at 23.4°N (within the red box in Fig. 2b) for **a** relative vorticity (shaded; $\times 10^{-4}$ s^{-1}) and updraft (contours; Pa s^{-1}), and for **b** Equivalent potential temperature (shaded; K), zonal wind component along with vertical velocity (vector; m s^{-1}) and divergence (contours; $\times 10^{-5}$ s^{-1}) **c** Skew-T log-P sounding, wind barbs (in kt) and hodograph at point 23.4°N, 88.4°E for 1200 UTC on 25 May 2021

at 1200 UTC on 25 May 2021 in Fig. 4c. The convective indices, i.e., the K index (George 1960) of 39 °C, the total totals index (TT; Miller 1972) of 41 °C, 6.87 cm of precipitable water (PW), the lifted index (LI; Galway 1956) of -3 and θe of 369 K indicate the favorable unstable conditions for the occurrence of a severe thunderstorm. The values of total wind shear from 0–6 km (~ 500 hPa) above ground level (AGL) and the bulk shear between 0–6 km (BSHR6) are calculated and found at 37 m s^{-1} and 16 m s^{-1}, respectively. The hodograph, representing the shear vector, shows a curved nature in the lowest 0–1 km (~ 850 hPa) and a straight line above it. The estimated strong values of vertical shear that veer clockwise are exceeded the limit of threshold values for developing supercells (Bunkers 2002). The moderate value of 1504 J kg^{-1} for CAPE, storm-relative environmental helicity (SREH; Davies-Jones et al. 1990) of 232 m^2 s^{-2} between 0–3 km (~ 700 hPa) AGL, environmental helicity (EH) of 302 m^2 s^{-2} and the bulk Richardson number (BRN) of 30 (Weisman and Klemp 1982) confirm the existence of supercell containing the rotating updraft.

All characteristics indicate a shallow mesocyclone associated with a mini supercell (Burgess et al. 1995; Suzuki et al. 2000) though high-resolution spatial and temporal data are needed to specify the characteristics of the tornado. In addition, the calculated energy helicity index (EHI; Hart and Korotky 1991) is found to have a value of 2.2 indicating the WB tornado is strong with a strength equivalent to EF2–3 based on the Enhanced Fujita (EF) scale. Mentionable that the operational significances of all convective parameters are available in Grieser (2012).

3.2 Anticipated Tornadoes for Inland Cyclone Yaas (2021)

Using the ECMWF-IFS analysis data, the environment for possible tornadoes coupled with the TC system is further analyzed at 6-h intervals by some significant atmospheric parameters when the TC crosses over the land. For example, the environment at 0000 UTC on 27 May 2021, the time after one day from the landfall of the TC center, is displayed in Fig. 5 to understand the possibility of a multi-day outbreak of tornadoes. Therefore, the key atmospheric ingredients that lead to the development of tornadoes in the environment of landfalling TC are investigated below.

Bulk shear between 0–1 km AGL (BSHR1) The low-level vertical wind shear is the fundamental potential environment supporting the development of tornadoes with supercell storms (Brooks and Craven 2002). Figure 5a shows the distribution of BSHR1 and indicates that when Cyclone Yaas (2021) makes landfall and begins decaying, the ambient winds at the surface die off quicker than the winds at 850 hPa resulting in a

low-level shear of > 15 m s^{-1} over the land. Strong low-level shear is noticed in the right-front quadrant of the TC due to existing of intense 850-hPa wind (> 25 m s^{-1}) on the northeastern side of the TC center (Fig. 5a).

SREH in the 0–1 km AGL (SREH1) The SREH1 is representative of streamwise vorticity within the storm inflow layer, which is calculated in the lowest one km for predicting tornadoes. The following equation (Markowski and Richardson 2010) is used for computing the low-level SREH and the result is displayed in Fig. 5b.

$$SREH = \sum_{n=1}^{N-1} \left[(u_{n+1} - c_x)(v_n - c_y) - (u_n - c_x)(v_{n+1} - c_y) \right]$$

where u and v are the environmental wind speed components, c_x and c_y are the components of storm motion and the height level $n = 1$ to N.

The horizontal distributions of SREH1 shown in Fig. 5b exhibit the large values within a wide area and the greater values of 300 m^2 s^{-2} indicate the possibility of having tornadoes rated EF2–3 in the northeast of the TC center.

EHI in the 0–1 km AGL The EHI represented by the combination of instability and SREH for understanding the energy of the convection is shown in Fig. 5b. The index values of ≥ 1 are prominent also in the northeastern side of the TC, specifying the existence of significant tornadoes in the supercells.

Significant tornado parameter (STP) The STP is a widely used composite index initially designed by Thompson et al. (2003), combining several variables supportive of evolving a tornado. The index includes BSHR6, SREH1, surface- based CAPE (sbCAPE), and surface-based lifting condensation level (sbLCL), which is formulated for fixed layer as

$$STP = \left(\frac{sbCAPE}{1500 \ Jkg^{-1}} \right) \left(\frac{2000 - sbLCL}{1000m} \right) \left(\frac{SREH1}{150 \ m^2 s^{-2}} \right) \left(\frac{BSHR6}{20 \ ms^{-1}} \right)$$

Figure 5c represents the STP to find out the spatial location susceptible to form tornadoes connecting to inland Cyclone Yaas (2021), one day after touching the land. The strong values of STP ≥ 3 indicate that the areas in West Bengal, India and Bangladesh are more vulnerable to have intense tornadoes (rated EF2 or greater) associated with supercell thunderstorms in the rainbands of the TC.

Potential vorticity (PV) anomalies Concerning the distributions of low-level shear, helicity, EHI and STP, the four locations (A–D in Fig. 5c) are randomly chosen to be expected as tornadoes. The distance in each location from the TC center is considered greater than 250 km to avoid the influence of the center vortex. The Ertel's PV (Schubert et al. 2004) is diagnosed in pressure (p) coordinates for each location to
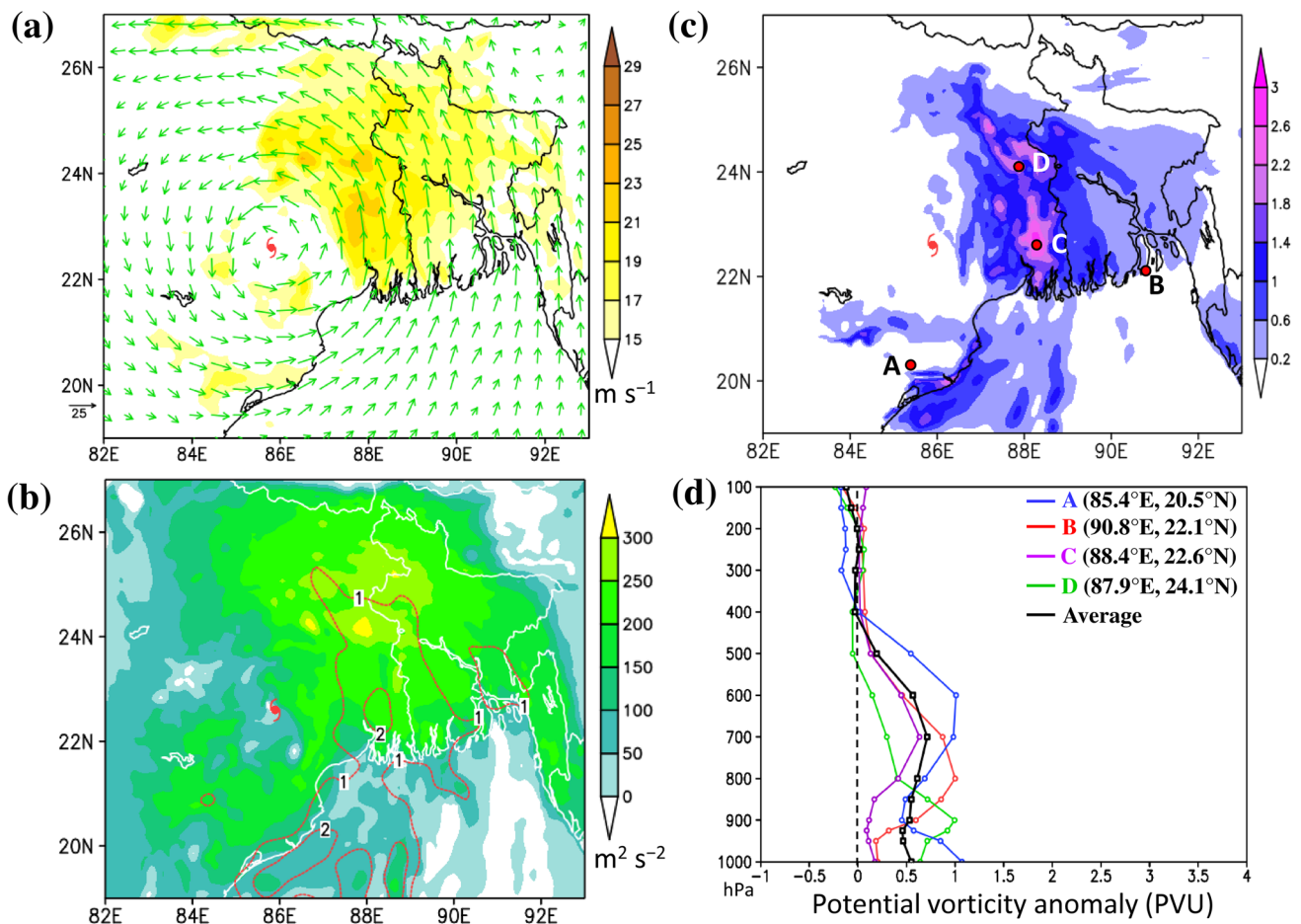
Fig. 5 a Bulk wind shear between 0–1 km (shaded; m s^{-1}) and wind speed (vector; m s^{-1}) at 850 hPa **b** 0–1-km storm relative environmental helicity (shaded; m^2 s^{-2}) and energy helicity index (contours) **c** Significant tornado parameter (STP) **d** PV anomaly vs height for the locations A–D (indicated in Fig. 5c) at 0000 UTC on 27 May 2021

understand the vorticity dynamics on the storm-scale including thermodynamical processes. The PV expression represents a product of absolute vorticity on an isentropic surface and thermodynamic stability, which is shown below.

$$PV = -g(\zeta + f)\frac{\partial \theta}{\partial p}$$

where g, ζ, f and θ are the gravitational acceleration, relative vorticity, Coriolis parameter and potential temperature, respectively.

Figure 5d displays the vertical distribution of PV anomalies calculated from the average area of 2°×2° centering each location. The positive PV anomalies from surface to 400 hPa for all cases identify cyclonic vorticity and high static stability. The maximum PV is found in the mid-troposphere at around 700 hPa with an average value of 0.8 PVU (1 PVU = 10^{-6} K m^2 kg^{-1} s^{-1}). A significant near-surface cyclonic PV anomaly (0.5 PVU on average) indicates the presence of a cloud-scale vortex at the low level or existence of tornadoes even after one day from the landfall of Cyclone Yaas (2021).

4 Discussion and Concluding Remarks

The environment with strong lower-tropospheric vertical wind shear, moderate SREH and limited instability for the WB tornado is found similar to that associated with the tornadoes for landfalling TCs explained by McCaul (1991) for the period 1948–1986. The environment of Cyclone Yaas (2021) also remains supportive of the outbreak of multiple tornadoes in the multi-days period after its landfall. The tornadoes are particularly favorable in the right-front quadrant of the TC with an intensity of EF2–3. The TC-tornadoes are likely to be produced from mini-supercells or shallow supercells (Suzuki et al. 2000) due to the existence of weak low-level cold pools in the moist environment of the TCs (McCaul and Weisman 1996). Mini supercells are short-lived, smaller in dimension, less intense and contain shallow mesocyclones, in contrast to typical midlatitude supercells (Moller et al. 1994). However, it is evident that both the mini-supercells and classical supercells were developed in the rainbands of Cyclone Sidr (category-5 cyclone) formed

in 2007 when it was over the BoB (Akter and Tsuboki 2010). Even if the occurrence of classical supercells is not precisely the same for cyclone Yaas, there is scope for similar insights to that of Sidr and other TCs. The present study gives a potential indication in this direction. However, due to a lack of high-resolution spatial and temporal data, this study limits the detailed structure and evolution of supercells embedded in the rainbands of Cyclone Yaas and corresponding tornadoes which could be ascertained using cloud-resolving simulation in further research.

The tornadoes integrated with TCs over the Atlantic and Pacific Ocean basins are well-reported and predicted. In contrast, TC-tornadoes connected to the North Indian Ocean (or the BoB) are still unfamiliar to ordinary people due to limited understanding and lack of research. As tornadoes can form inland far from TC centers as cyclone Yaas, intensive close monitoring and tracking of the path of tornadic-supercell thunderstorms are time demanding needs to minimize the damage to properties and loss of life in the highly populated littoral counties of the BoB.

Data Availability The data used in the present study were taken from IMD best track data, which is available in https://rsmcnewdelhi.imd.gov.in/report.php?internal_menu=MzM=. Also ECMWF IFS CY41r2 high-resolution data were used from https://rda.ucar.edu/datasets/ds113.1/ (anyone can access the data through free registration).

Declarations

Ethical Approval This article does not contain any studies with human participants or animals performed by the author. It also has not been published by another journal.

Conflict of Interest The authors declare that they have no conflict of interest.

References

Akter, N.: Mesoscale convection and bimodal cyclogenesis over the Bay of Bengal. Mon. Wea. Rev. **143**, 3495–3517 (2015). https://doi.org/10.1175/MWR-D-14-00260.1

Akter, N., Tsuboki, K.: Characteristics of supercells in the rainband of numerically simulated cyclone Sidr. SOLA. **6A**, 25–28 (2010). https://doi.org/10.2151/sola.6A-007

Assessment Capacities Project (ACAPS): India: Cyclone Yaas. Briefing note, pp. 1–3. https://www.acaps.org/sites/acaps/files/products/files/20210601_acaps_start_briefing_note_india_cyclone_yaas.pdf (2021) Accessed 17 July 2021

Bikos, D., Finch, J., Case, J.L.: The environment associated with significant tornadoes in Bangladesh. Atmos. Res. **167**, 183–195 (2016). https://doi.org/10.1016/j.atmosres.2015.08.002

Brooks, H.E., Craven, J.P.: A database of proximity soundings for significant severe thunderstorms, 1957–1993. Preprints, 21st Conference on Severe Local Storms, pp. 643–646. American Meteorological Society, San Antonio, Texas (2002)

Bunkers, M.J.: Vertical wind shear associated with left-moving supercells. Wea. Forecasting. **17**, 845–855 (2002). https://doi.org/10.1175/1520-0434(2002)017<0845:VWSAWL>2.0.CO;2

Burgess, D.W., Lee, R.R., Parker, S.S., Floyd, D.L.: A study of mini supercells observed by WSR-88D radars. Preprints, 27th Conference on Radar Meteorology, pp. 4−6. American Meteorological Society, Vail, CO (1995)

Davies-Jones, R., Burgess, D., Foster, M.: Test of helicity as a forecast parameter. Preprints, 16th Conf. on severe local storms, pp. 588–592. American Meteorological Society, Kananaskis Park, AB, Canada (1990)

Fujita, T.T., Watanabe, K., Tsuchitya, K., Shimada, M.: Typhoon-associated tornadoes in Japan and new evidence of suction vortices in a tornado near Tokyo. J. Meteorol. Soc. Jpn. **50**, 431–453 (1972). https://doi.org/10.2151/jmsj1965.50.5_431

Galway, J.G.: The lifted index as a predictor of latent instability. Bull. Am. Meteorol. Soc. **37**, 528–529 (1956). https://doi.org/10.1175/1520-0477-37.10.528

George, J.J.: Weather forecasting for aeronautics. Academic, New York (1960)

Grieser, J.: Convection parameters. Selbstverl, Germany (2012)

Hart, J.A., Korotky, W.: The SHARP workstation v1.50 users guide. pp. 30. NOAA, U.S. Department of Commerce, National Weather Service (1991)

India Blooms, India: Ahead of Cyclone Yaas, 2 people electrocuted in Bengal Tornado, 40 houses destroyed. https://www.indiablooms.com/news-details/N/72356/ahead-of-cyclone-yaas-2-people-electrocuted-in-bengal-tornado-40-houses-destroyed.html (2021) Accessed 17 July 2021

International Federation of Red Cross and Red Crescent Societies (IFRC): Bangladesh: Cyclone Yaas. Operation Update Report, pp. 1–18. https://reliefweb.int/sites/reliefweb.int/files/resources/MDRBD027du1.pdf (2021) Accessed 17 July 2021

Koch, E., Koh, J., Davison, A.C., Lepore, C., Tippett, M.K.: Trends in the extremes of environments associated with severe U.S. thunderstorms. J. Clim. **34**, 1259–1272 (2021). https://doi.org/10.1175/JCLI-D-19-0826.1

Malardel, S., Wedi, N., Deconinck, W., Diamantakis, M., Kuhnlein, C., Mozdzynski, G., Hamrud, M., Smolarkiewicz, P.: A new grid for the IFS. Newsletter No. 146 - Winter 2015/16, pp. 23–28. European Centre for Medium-Range Weather Forecasts, Reading (2015). https://data.ucar.edu/en/dataset/ecmwf-ifs-cy41r2-high-resolution-operational-forecasts. Accessed 12 June 2021

Markowski, P., Richardson, Y.: Mesoscale meteorology in the midlatitudes. Wiley-Blackwell, Hoboken (2010)

McCaul, E.W., Jr: Buoyancy and shear characteristics of hurricane-tornado environments. Mon. Wea. Rev. **119**, 1954–1978 (1991). https://doi.org/10.1175/1520-0493(1991)119<1954:BASCOH>2.0.CO;2

McCaul, E.W., Jr, Weisman, M.L.: Simulations of shallow supercell storms in landfalling hurricane environments. Mon. Wea. Rev. **124**, 408–429 (1996). https://doi.org/10.1175/15200493(1996)124<0408:SOSSSI>2.0.CO;2

Miller, R.C.: Notes on analysis and severe-storm forecasting procedures of the air force global weather Central. Weather Service Tech. Rep. 200 (Rev.), pp. 190. Scott Air Force Base, IL, Air Weather Service (1972)

Mills, G.A., Colquhoun, J.R.: Objective prediction of severethunderstorm environments: preliminary results linking a decsion tree with an operational NWP model. Wea. Forecasting **13**, 1078–1092 (1998). https://doi.org/10.1175/1520-0434(1998)013<1078:OPOSTE>2.0.CO;2

Moller, A.R., Doswell, C.A., Foster, M.P., Woodall, G.R.: The operational recognition of supercell thunderstorm environments and storm structures. Wea. Forecasting. **9**, 327–347 (1994). https://doi.org/10.1175/1520-0434(1994)009<0327:TOROST>2.0.CO;2

Moore, T.W., Dixon, R.W.: A spatiotemporal analysis and description of Hurricane Ivan's (2004) tornado clusters. Pap. Appl. Geogr. **1**, 192–196 (2015). https://doi.org/10.1080/23754931.2015.1012449

Moore, T.W., Sokol, N.J., Blume, R.A.: Spatial distributions of tropical cyclone tornadoes by intensity and size characteristics. Atmosphere **8**, 160 (2017). https://doi.org/10.3390/atmos8090160

Novlan, D.J., Gray, W.M.: Hurricane-spawned tornadoes. Mon. Wea. Rev. **102**, 476–488 (1974). https://doi.org/10.1175/1520-0493(1974)102<0476:HST>2.0.CO;2

Ono, Y.: Climatology of tornadoes in Bangladesh, 1990–1994. J. Meteorol. **22**, 325–340 (1997)

Orlanski, I.: A rational subdivision of scales for atmospheric processes. Bull. Am. Meteorol. Soc. **56**, 527–530 (1975)

Schubert, W., Ruprecht, E., Hertenstein, R., Ferreira, R.N., Taft, R., Rozoff, C., Ciesielski, P., Kuo, H.-C.: English translations of twenty-one of Ertel's papers on geophysical fluid dynamics. Meteorol. Z. **13**, 527–576 (2004). https://doi.org/10.1127/0941-2948/2004/0013-0527

Suzuki, O., Niino, H., Ohno, H., Nirasawa, H.: Tornado producing mini supercells associated with Typhoon 9019. Mon. Wea. Rev. **128**, 1868–1882 (2000). https://doi.org/10.1175/15200493(2000)128<1868:TPMSAW>2.0.CO;2

The Hindustan Times, India: Mini tornado hits villages of West Bengal before cyclone. https://www.Hindustantimes.com/cities/kolkata-news/mini-tornado-hits-villages-of-west-bengal-before-cyclone-101622068150190.html (2021) Accessed 17 July 2021

Thompson, R.L., Edwards, R., Hart, J.A., Elmore, K.L., Markowski, P.: Close proximity soundings within supercell environments obtained from the Rapid Update Cycle. Wea. Forecasting. **18**, 1243–1261 (2003). https://doi.org/10.1175/15200434(2003)018<1243:CPSWSE>2.0.CO;2

Weisman, M.L., Klemp, J.B.: The dependence of numerically simulated convective storms on vertical shear and buoyancy. Mon. Wea. Rev. **110**, 504–520 (1982). https://doi.org/10.1175/15200493(1982)110<0504:TDONSC>2.0.CO;2

Weisman, M.L., Trapp, R.J.: Low-level mesovortices within squall lines and bow echoes. Part I: Overview and sensitivity to environmental vertical wind shear. Mon. Wea. Rev. 131, 2779–2803 (2003). https://doi.org/10.1175/1520-0493(2003)131<2779:LMWSLA>2.0.CO;2

Weiss, S.J.: On the operational forecasting of tornadoes associated with tropical cyclones. Preprints, 14th Conference on Severe Local Storms, pp. 293–296. Indianapolis, IN, USA (1985)

Yamane, Y., Hayashi, T., Dewan, A.M., Akter, F.: Severe local convective storms in Bangladesh: Part I Climatology. Atmos. Res. **95**, 400–406 (2009). https://doi.org/10.1016/j.atmosres.2009.11.004